

Helen T. Winer-Muram, MD  
 John M. Boone, PhD  
 Haywood L. Brown, MD  
 S. Gregory Jennings, MD  
 William C. Mabie, MD  
 Gerard T. Lombardo, MD

**Index terms:**

Embolism, pulmonary, 60.72  
 Pregnancy, 85.131, 85.47  
 Radiations, exposure to patients and personnel  
 Thorax, CT, 60.1211, 60.12115

**Published online before print**  
 10.1148/radiol.2242011581  
**Radiology 2002; 224:487-492**

**Abbreviations:**

DVT = deep venous thrombosis  
 PE = pulmonary embolism  
 V-P = ventilation-perfusion

<sup>1</sup> From the Department of Radiology, Indiana University School of Medicine, 550 N University Blvd, Indianapolis, IN 46202 (H.T.W.M., S.G.J.); Department of Radiology, University of California-Davis Medical Center, Sacramento (J.M.B.); Department of Obstetrics and Gynecology, St Vincent's Medical Center, Indianapolis, Ind (H.L.B.); Department of Obstetrics and Gynecology, University of Tennessee College of Medicine, Memphis (W.C.M.); and Division of Pulmonary Medicine and Critical Care, New York Methodist Hospital, Brooklyn, NY (G.T.L.). Received September 24, 2001; revision requested November 27; revision received December 17; accepted January 22, 2002. **Address correspondence to** H.T.W.M. (e-mail: hwinermu@iupui.edu).

© RSNA, 2002

**Author contributions:**

Guarantor of integrity of entire study, H.T.W.M.; study concepts, G.T.L.; study design, H.T.W.M., J.M.B.; literature research, H.T.W.M., J.M.B.; clinical studies, H.L.B.; experimental studies, J.M.B.; data acquisition, H.L.B., J.M.B.; data analysis/interpretation, H.T.W.M., J.M.B., S.G.J.; statistical analysis, J.M.B.; manuscript preparation, S.G.J., H.T.W.M.; manuscript definition of intellectual content, H.T.W.M., J.M.B.; manuscript editing, J.M.B., H.T.W.M., S.G.J.; manuscript revision/review, S.G.J., H.T.W.M., W.C.M.; manuscript final version approval, H.T.W.M.

## Pulmonary Embolism in Pregnant Patients: Fetal Radiation Dose with Helical CT<sup>1</sup>

**PURPOSE:** To calculate mean fetal radiation dose from helical chest computed tomography (CT) by using maternal-fetal geometries obtained from healthy pregnant women and to compare the calculated CT doses with the fetal doses reported with scintigraphy.

**MATERIALS AND METHODS:** Maternal-fetal geometries were determined in 23 pregnant women with varying body mass index and fetal gestational age. Monte Carlo techniques were used to estimate the dose that would be received by each fetus from CT scanning performed with the following parameters: 120 kVp; 100 mA; scanning time, 1 second per section; collimation, 2.5 mm; pitch of 1. Craniocaudal extent of the scan was 11 cm, with the most caudal section edge being 5 mm inferior to the xiphoid process.

**RESULTS:** For helical CT, estimated mean fetal doses in micrograys at varying gestational ages were as follows: 3.3–20.2  $\mu$ Gy, first trimester; 7.9–76.7  $\mu$ Gy, second trimester; and 51.3–130.8  $\mu$ Gy, third trimester. These values were all less than mean fetal doses reported with scintigraphy, with 37–74 MBq of macroaggregates of human serum albumin labeled with technetium 99m. If 200 mAs (pitch of 1.8) was used, the mean fetal doses were still less than those with scintigraphy.

**CONCLUSION:** The average fetal radiation dose with helical CT is less than that with ventilation-perfusion lung scanning during all trimesters.

© RSNA, 2002

Venous thromboembolism is a leading cause of maternal mortality and has been reported to occur in 0.5–3.0 of 1,000 pregnancies (1,2). Pregnancy increases the risk of venous thromboembolism by a factor of five over that of a nonpregnant woman of similar age (3). Increased venous stasis is the most important factor, but prolonged bed rest, pregnancy-related hypercoagulability, decreased fibrinolysis, and familial predisposition are also implicated (4). While the risk of thrombosis has usually been considered greatest during the third trimester and immediately postpartum, there is evidence that venous thromboembolism may occur with almost equal frequency in all three trimesters (4).

The incidence of pulmonary embolism (PE) depends on whether deep venous thrombosis (DVT) has been treated adequately. Up to 24% of patients with untreated DVT develop PE, with a mortality rate of approximately 15% (5). Because venous thromboembolism is potentially preventable and treatable, early and accurate diagnosis and treatment are mandatory (6).

Several studies have provided guidelines for investigating PEs in pregnant patients who are suspected of having them. These guidelines attempt to balance diagnostic efficacy and minimization of fetal exposure to ionizing radiation (6–8). Ventilation-perfusion (V-P) lung scanning is still considered to be the primary diagnostic tool for PE in pregnant women (9,10). By using 37–74 MBq of macroaggregates of human serum albumin labeled with technetium 99m, the fetal dose from lung scanning is approximately 100–370  $\mu$ Gy, a relatively low exposure for the fetus (7,8).

Although helical CT is being used more and more to diagnose PE, there are questions about the safety of its use during pregnancy. The purpose of this study was to calculate the

mean fetal radiation dose from helical chest CT by using maternal-fetal geometries obtained from healthy pregnant women and to compare the calculated CT doses with the reported fetal doses with scintigraphy.

## MATERIALS AND METHODS

### Clinical Data

Institutional review board approval with waiver of informed consent was obtained. From July 2001 to August 2001, 23 consecutive healthy pregnant patients of one author (H.L.B.) were selected for measurement of maternal-fetal geometry. Maternal age, height, and weight and fetal gestational age (estimated by using ultrasonography [US]) were noted (H.L.B.). For pregnant patients with less than 13 weeks gestation, the uterine dimensions were measured with US that incorporated the entire uterine volume. The length was measured by using transvaginal and transabdominal US to obtain the most accurate uterine, or fetal, dimensions. The measurement was from the top of the fundus of the uterus to the level of the internal os of the cervix.

Transverse dimensions were measured at the widest point of the uterus. The top of the uterus, or fundal height, was marked, and the distance from the xiphoid process to the fundus was measured. Measurements in patients with more than 13 weeks gestation were performed with standard techniques. The top of the fundus of the uterus was again marked by using transabdominal US and measured down to the pubic symphysis and up to the xiphoid process. The widest uterine measurement was obtained by marking the maximum outer width on both sides of the umbilicus by using US and then was measured from mark to mark. Geometric assumptions for the Monte Carlo studies are discussed later.

The following CT protocol was used for calculations: 120 kVp, 100 mAs, 2.5-mm section interval, 11-cm craniocaudal distance, pitch of 1. This distance is generally sufficient to extend from just inferior to the xiphoid process to the aortic arch. With this protocol, the mean fetal doses were calculated by using Monte Carlo techniques in the 23 study patients.

### Monte Carlo Calculations

The circumference in each of the 23 women was measured physically, but for the Monte Carlo studies we also needed to obtain an estimate of the relative shape of a patient at the xiphoid process.

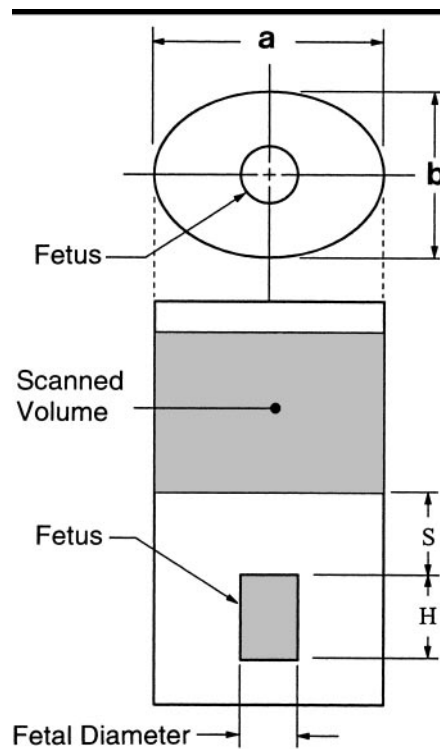


**Figure 1.** Drawing illustrates the geometry used in the Monte Carlo calculations. The mother was modeled as an ellipse with a mean eccentricity of 0.68. The specific dimensions ( $a$  and  $b$ ) were determined by measuring the circumference of the mother. The fetus was modeled as a right cylinder, where the fetal diameter, fetal height ( $H$ ), and distance from the top of the fetus to the scanned volume ( $S$ ) were individually measured by using US.

Assuming an ellipsoidal cross section, we computed the eccentricity from a number of CT scans. CT scans that were acquired as a part of clinical care in 21 consecutive nonpregnant women (mean age, 50.6 years; SD, 17.8) were evaluated. Coronal and sagittal diameters at the level of the xiphoid process were determined by using quantitative measurement software (E-Film; E-Film, Toronto, Ontario, Canada). This analysis of existing patient data was performed with a protocol approved by the institutional review board at University of California-Davis Medical Center, Sacramento, with waiver of informed consent.

An elliptical cross section was assumed, and the eccentricity of each patient at the level of the xiphoid process was calculated on the basis of image-based measurements of the thickness and width of the patient. The mean eccentricity and the median eccentricity were 0.68 and 0.66, respectively (Fig 1). Since the mean age of this group was substantially higher than that of the study group, the eccentricity was evaluated

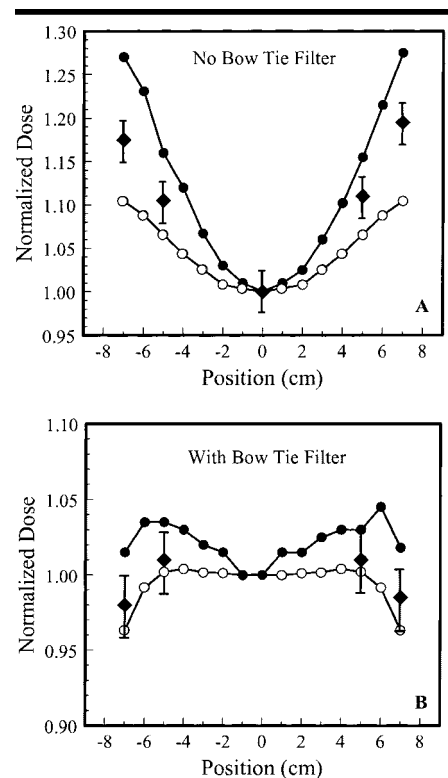


**Figure 2.** Graphs show a comparison of the results of this study ( $\circ$ ) with the physically measured results ( $\blacklozenge$ ) and the results derived by means of the EGS4 Monte Carlo calculations ( $\bullet$ ) as reported by Caon et al (14). The x axis refers to the location along a diameter within a cylindrical phantom, with the position of  $x = 0$  cm being at the center. *A*, Moderate agreement is seen with no bow tie filter. *B*, Excellent agreement between the SIERRA-derived results and the measured data of Caon et al (14) is seen with the bow tie filter in place. The bow tie filter was used in the development of the pediatric dose values in this study.

as a function of patient age by using linear regression. Only a slight dependence was found, and, therefore, the mean eccentricity value was used for all 23 pregnant women modeled in the Monte Carlo calculations. Although the eccentricity measurements were obtained in nonpregnant women, the shape of a woman at the level of the thoracic cavity changes only slightly during pregnancy, and, thus, we thought that the eccentricity measurement determined in this group would be reasonably reflective of the pregnant patient.

Monte Carlo techniques were used to compute the radiation doses that the fetuses would have received if the patients had undergone chest CT with the parameters previously described. The initial CT section (section 1) was positioned with the inferior edge of the scan 5 mm below the xiphoid process, and the dose com-

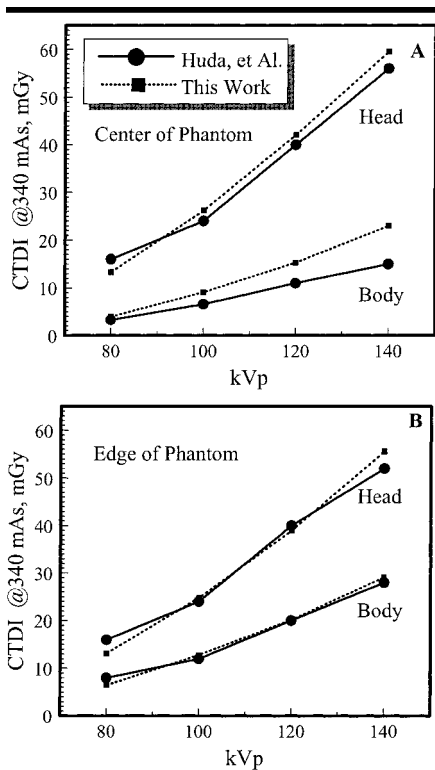


**Figure 3.** Graphs show a comparison of CT dose index (*CTDI*) data determined in this study and of the values reported by Huda et al (15). The values determined at the center of the plastic (polymethylmethacrylate) phantom are shown in *A*, and the values determined at the edge of the phantom are illustrated in *B*. The head phantom is a 16-cm-diameter plastic cylinder, and the body phantom is a 32-cm-diameter plastic cylinder.

putations included the contribution of an additional 43 (for a total of 44) 2.5-mm-thick, contiguous, transverse (non-helical) sections. The dose distribution as modeled was virtually identical to that of a helical CT study with a pitch of 1, with the same scanning volume. This geometry is equivalent to the acquisition of CT sections along a craniocaudal axis of 11 cm, regardless of the combination of section thickness or image numbers. For example, the dose associated with 44 2.5-mm sections is equivalent to that associated with 37 3-mm, 22 5-mm, or 11 10-mm sections, as long as the scanned volume (in relative position to the fetus) and other CT parameters remain the same.

Previously validated simple investigational environment for radiology research applications, or SIERRA, Monte Carlo techniques were used for this study (11,12), and additional validation efforts were also performed. The Monte Carlo code propagated 22 million x-ray pho-

tons per patient. Photoelectric, Compton, and Rayleigh scattering interactions were modeled with the energy range of 1–150 keV. Energy deposition was determined in water-equivalent ellipsoid (mathematic) phantoms by using the geometries of each of the 23 study patients. The same eccentricity (mean, 0.68) was assumed for each patient.

The x-ray output data of a commercially available CT scanner (CT/i; GE Medical Systems, Milwaukee, Wis) were used to relate milliamperere seconds to photon fluence. The normalized output (milliroentgens per milliamperere seconds at isocenter versus kilovolt peak) of a scanner was measured by using an exposure meter (MDH 1015; Radcal, Monrovia, Calif) and a 3-cm<sup>3</sup> CT pencil chamber. By using a physical scale drawing of an actual beam-shaping filter. The projection thickness of an actual beam-shaping filter was measured on a scale drawing with a ruler and protractor as a function of fan angle, and the thickness was computer fit as a function of angle. The filter composition was synthetic resin (Teflon) (C<sub>2</sub>F<sub>4</sub>), with a density of 2.2 g/cm<sup>3</sup>. The x-ray attenuation of the beam-shaping filter was used to modify the photon distribution in the plane of the fan angle. A source-to-isocenter distance of 63 cm was used. The x-ray spectrum was generated by using a spectral model (13), and a half-value layer of 8.2 mm of aluminum was achieved by filtering the native spectrum with 8.0 mm of aluminum. This half-value layer matched that measured with a clinical scanner at 120 kVp at University of California-Davis Medical Center.

A Monte Carlo simulation was performed in each patient by using the measurements for each maternal-fetal geometry. The axial diameter and craniocaudal length were used to simulate the fetus as a right cylinder at the center of the ellipse that was used to define the mother's geometry (Fig 1). The energy deposited in this cylindrical simulated fetus of water-equivalent unit-density material was used for calculating the dose. The assumption of a cylindrical shape for the fetus facilitates the Monte Carlo computation of dose to this region.

Differences in shape between a cylinder and the actual fetus have only a small effect on the fetal dose calculation, as long as the cylinder dimensions simulate the bounds of the fetus. The US-based anatomic measurements were performed to accurately determine these distances. In each woman, the measured circumference at the xiphoid process was used to determine the dimensions of each elliptic

semiaxis (values *a* and *b* in Fig 1). In addition to calculation of the mean fetal dose, determination of the maximum fetal dose was performed in a separate series of Monte Carlo experiments. The maximum fetal dose was estimated by means of calculating the dose to the uppermost 1 cm of the fetus (the portion closest to the scanned volume).

## RESULTS

### Monte Carlo Comparisons

Results were reported for the 120-kVp spectrum, in which the output was measured as 19.70 mR/mAs (air kerma, 0.172 mGy/mAs) at the isocenter of the scanner. Figure 2 illustrates SIERRA Monte Carlo results compared with the reported data of Caon et al (14) and shows both their physically measured and Monte Carlo-derived results that are based on the EGS4 code. Results were calculated both with (Fig 2, *A*) and without (Fig 2, *B*) a beam-shaping filter. Figure 3 illustrates the CT dose index calculated by using the SIERRA code with the same conditions as those reported by Huda et al (15).

The CT dose index data are compared at the center of the cylindric plastic phantom (Fig 3, *A*) and at its edge (Fig 3, *B*) for both the head phantom (16 cm diameter) and the body phantom (32 cm diameter). For purposes of comparison with other CT dose index values, the scanner that was simulated in this investigation produced a CT dose index multiple scan average dose of 4.50 mGy per 100 mAs at the center of a 32-cm-diameter plastic phantom and a CT dose index MSAD of 5.93 mGy per 100 mAs at the edge of the phantom. Because penumbra cutoff effects were not included in this simulation, the CT dose index values from real multisection CT scanners should be slightly higher than these values.

### Fetal Dose Assessment

Maternal and fetal measurements are presented in Table 1. Eight patients were in the first trimester, nine were in the second trimester, and six were in the third trimester. Mean maternal age was 31 years (SD, 6.7).

The mean fetal dose was calculated for each patient for 44 individual 2.5-mm-thick CT scans (Fig 4). These exposure conditions are identical to those associated with 37 3-mm, 22 5-mm, or 11 10-mm-thick CT sections. An equation that corresponds to the best-fit line is shown in Figure 4. The equation was determined for 100 mAs and transverse scans; for dif-

**TABLE 1**  
**Characteristics of Study Population**

Patient No.	Maternal Age (y)	Maternal Weight (lb)*	Maternal Height (inch)†	Maternal Body Mass Index	Fetal Gestational Age (wk)	Maternal Xiphoid Circumference (cm)	Xiphoid-Fetus Distance (cm)	Fetal Height (cm)	Fetal Width (cm)
First Trimester									
1	33	135	63	24.0	8	77	24	8	9
2	36	135	68	20.6	8	88	30	8	8
3	36	182	67	28.6	9	86	27	8	6
4	21	163	64	28.0	10	85	29	7	8
5	29	127	65	21.2	11	77	22	9	8
6	38	209	67	32.8	11	91	27	12	9
7	43	133	67	20.9	12	79	21	7	8
8	33	120	63	21.3	12	78	19	12	11
Second Trimester									
9	19	133	67	20.9	13	79	21	7	8
10	36	228	66	36.9	16	103	19	18	16
11	40	140	66	22.6	18	77	17	14	14
12	22	154	65	25.7	18	80	23	14	12
13	34	145	64	24.9	19	88	17	16	15
14	26	136	68	20.7	21	76	11	17	14
15	24	110	62	20.2	23	73	15	22	16
16	37	180	68	27.4	24	87	14	21	22
17	22	185	63	32.8	27	96	17	26	24
Third Trimester									
18	27	135	64	23.2	30	82	10	27	21
19	32	188	66	30.4	31	91	9	32	23
20	27	182	68	27.7	34	95	6	33	27
21	26	143	62	26.2	35	65	6	32	26
22	27	134	57	29.1	37	87	4	34	26
23	35	195	69	28.9	37	91	7	37	31

\* To convert to kilograms, multiply by 0.45.

† To convert to centimeters, multiply by 2.54.

ferent milliamper second values and helical acquisition with pitches other than 1.0, the values generated by the equation should be adjusted. The actual fetal dose varies linearly with the milliamper second values; for example, if 200 mAs is used, the fetal dose is multiplied by 200 divided by 100. For helical acquisition, the dose is additionally multiplied by the factor 1/pitch. Mean fetal doses were compared with reported (8) doses delivered with scintigraphy (Table 2).

With cranial-to-caudal progression, the dose to the fetus decreases exponentially. Near the caudal end of the fetus, very small doses are received, and these small doses substantially lower the mean fetal dose. Because of this bias, the maximum fetal dose was also computed (Fig 5) (Table 2). The maximum fetal dose is experienced by the uppermost 1 cm of the fetus, or that portion closest to the scanned volume.

## DISCUSSION

In all three trimesters, the mean fetal dose delivered with helical CT (120 kVp, 100

mAs, pitch of 1) is less than that delivered with V-P scanning. In 20 of our 23 study patients, the mean fetal dose was less than 60  $\mu$ Gy, the mean fetal dose described by Sharp et al (16). For different CT parameters or scanning volumes, with a specific maternal-fetal geometry, the maximum fetal dose can be calculated as demonstrated in Figure 5. The doses in Table 2 do not include additional exposure from a scanogram. Because the helical CT scan begins near an anatomic landmark (the xiphoid process), we believe that a scanogram is not necessary (17).

Numerous studies have been published in which the researchers describe the value of helical CT for PE diagnosis, and findings in most show that helical CT is an accurate tool for diagnosis of PE in main, lobar, and segmental pulmonary arteries. For emboli in these sites, helical CT is approximately 90% sensitive (range, 60%–100%) and 90% specific (range, 80%–100%) (18). Helical CT also has been reported (19) to demonstrate excellent interobserver agreement. However, helical CT is less accurate for imaging peripheral emboli in subsegmental vessels.

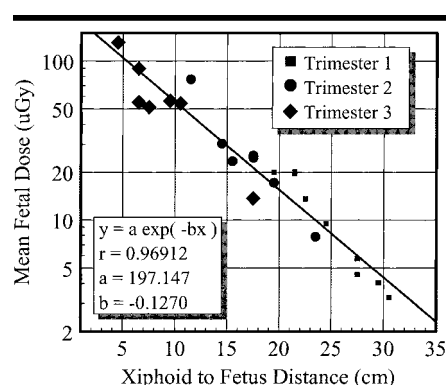


**Figure 4.** Graph shows the mean fetal dose for each of 23 patients. These data were determined by summing the dose contribution from each of the 44 CT sections in the study.

When all pulmonary vessels are included, the sensitivity and specificity of helical CT for the diagnosis of PE range from 53%–100% and 75%–100%, respectively (18). Poor contrast opacification, motion artifacts, or technical factors may cause 5%–10% of CT scans to be nondiagnostic (18). In addition, for diagnosis of PE, ad-

**TABLE 2**  
**Theoretic CT Doses**

Patient No.	Dose ( $\mu\text{Gy}$ )	
	Mean	Maximum
First trimester*		
1	9.5	17.4
2	3.3	6.4
3	5.7	10.9
4	4.1	7.0
5	13.6	26.9
6	4.6	10.8
7	20.2	34.1
8	20.0	50.1
Second trimester†		
9	19.7	33.8
10	17.2	51.1
11	25.5	71.9
12	7.9	21.9
13	24.7	75.8
14	76.7	259.5
15	23.5	100.5
16	30.4	119.9
17	13.7	64.4
Third trimester‡		
18	54.1	277.9
19	56.2	334.0
20	89.7	551.2
21	55.0	365.6
22	130.8	862.1
23	51.3	355.5

Note.—The values reported reflect the calculated values; however, the level of precision does not justify the use of four significant digits.

\* Dose range at scintigraphy was 104–296  $\mu\text{Gy}$  (data from Russell et al [8]).

† Dose range at scintigraphy was 148–370  $\mu\text{Gy}$  (data from Russell et al [8]).

ministration of intravenous contrast material is necessary. Although intravenous administration of nonionic contrast material during pregnancy is performed with other imaging studies (eg, head CT), and studies in pregnant animals have shown no evidence of harm to the fetus caused by nonionic contrast media (20), to our knowledge, no adequate and well-controlled studies have been performed in pregnant women.

Scintigraphy is the primary screening study in the assessment of PE in pregnant patients (9). However, V-P scans are usually not definitive in the diagnosis of acute PE; the presence or absence of PE is inconclusive in up to 80% of these scans (21). Most radiologists categorize abnormal lung scans into three classes according to the probability—low, intermediate, or high—that the finding is a PE. Even for a scan with a high probability, the sensitivity is only 41% (21). Thus, most patients with PE will have scans with intermediate or low probability. Moreover, prior episodes of PE may cause a false-positive result (21).

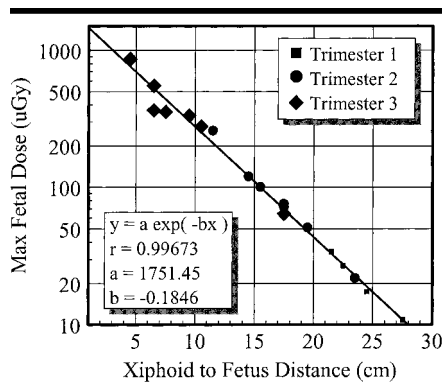


**Figure 5.** Graph shows the maximum dose per individual CT section for a 2.5-mm-thick, nonhelical, 120-kVp, 100-mAs scan. The data points correspond to the dose computed for the single highest-dose CT section in each of the 23 patients. In all cases, the highest dose was delivered to the CT section closest to the fetus.

Magnetic resonance (MR) imaging is an alternative to V-P scanning and helical CT because the fetus is not exposed to ionizing radiation or intravenous contrast material. Moreover, the sensitivity (90%) and specificity (77%) of MR are similar to those of helical CT for the diagnosis of PE (22). However, for this application, long acquisition times are needed, as well as respiratory and cardiac gating, and even then spatial resolution is relatively poor. Availability of this MR protocol is limited as well.

Because clinicians are reluctant to order additional imaging tests in pregnant women following an inconclusive V-P scan, we believe that it is important for them to recognize that helical CT is not only safe during pregnancy but also accurate for the diagnosis of PE in main, lobar, and segmental pulmonary arteries. Accurate diagnosis is critical, because there is substantial risk of morbidity to both mother and fetus from treatment. The recommended therapy for DVT and PE during pregnancy is intravenously administered heparin for 5–10 days, followed by subcutaneously administered heparin for the remainder of the pregnancy (4).

Postpartum therapy includes combined administration of heparin and warfarin initially, followed by administration of warfarin alone for 6 weeks or until at least 3 months of anticoagulation therapy have been completed (4). DVT prophylaxis must be considered during subsequent pregnancies, as the incidence of recurrent PE during each subsequent pregnancy is 4%–15% (23). Furthermore, a history of PE may preclude the future

use of oral contraceptives or hormonal replacement therapy (24).

Although it is desirable to limit fetal radiation exposure, a review of the literature suggests that in utero exposure of up to 50,000  $\mu\text{Gy}$  results in a negligible increase in the risk of childhood cancer (4,7). With careful use of available procedures, a diagnosis of PE can be made with exposures of less than 5,000  $\mu\text{Gy}$ . For example, even the combination of chest radiography (10  $\mu\text{Gy}$ ), V-P scanning (370  $\mu\text{Gy}$ ), helical CT scanning (131  $\mu\text{Gy}$ ), and pulmonary angiography with a brachial approach (500  $\mu\text{Gy}$ ) exposes the fetus to approximately 1,000  $\mu\text{Gy}$ . This dose is less than that received by the fetus from background radiation (eg, cosmic rays, radon, potassium 40) during the 9 months of pregnancy (1,150–2,550  $\mu\text{Gy}$ ) (25). By comparison, an exposure of at least 100,000  $\mu\text{Gy}$  is necessary before pregnancy termination is considered (26).

In summary, findings in this study show that the average fetal radiation dose with helical CT is less than that with V-P lung scanning during all trimesters. Pregnancy should not preclude use of helical CT for the diagnosis of PE.

#### References

1. Atrash HK, Rowley D, Hogue CJR. Maternal and perinatal mortality. *Curr Opin Obstet Gynecol* 1992; 4:61–71.
2. Barbour LA, Pickard J. Controversies in thromboembolic disease during pregnancy: a critical review. *Obstet Gynecol* 1995; 86:621–633.
3. Prevention of venous thrombosis and pulmonary embolism. NIH Consensus Development. *JAMA* 1986; 256:744–749.
4. Toggia MR, Weg JG. Venous thromboembolism during pregnancy. *N Engl J Med* 1996; 335:108–114.
5. Wessler S. Medical management of venous thrombosis. *Ann Rev Med* 1976; 27: 313–319.
6. Demers C, Ginsberg JS. Deep venous thrombosis and pulmonary embolism in pregnancy. *Clin Chest Med* 1992; 13:645–656.
7. Ginsberg JS, Hirsh J, Rainbow AJ, et al. Risks to the fetus of radiologic procedures used in the diagnosis of maternal venous thromboembolic disease. *Thromb Haemost* 1989; 61:189–196.
8. Russell JR, Stabin MG, Sparks RB, et al. Radiation absorbed dose to the embryo/fetus from radiopharmaceuticals. *Health Phys* 1997; 73:756–769.
9. Boiselle PM, Reddy SS, Villas PA, et al. Pulmonary embolus in pregnant patients: survey of ventilation-perfusion imaging policies and practices. *Radiology* 1998; 207:201–206.
10. Balan KK, Critchley M, Vedavathy KK, et al. The value of ventilation-perfusion imaging in pregnancy. *Br J Radiol* 1997; 70: 338–340.
11. Boone JM, Buonocore MH, Cooper VN. Monte Carlo validation in diagnostic ra-

- diological imaging. *Med Phys* 2000; 27: 1294–1304.
12. Boone JM, Cooper VN, Nemzek WR, McGahan JP, Seibert JA. Monte Carlo assessment of computed tomography dose to tissue adjacent to the scanned volume. *Med Phys* 2000; 27:2393–2407.
  13. Boone JM, Seibert JA. An accurate method for computer-generating tungsten anode x-ray spectra from 30 kV to 140 kV. *Med Phys* 1997; 24:1661–1670.
  14. Caon M, Bibbo G, Pattison J. A comparison of radiation dose measured in CT dosimetry phantoms with calculations using EGS4 and voxel-based computational models. *Phys Med Biol* 1997; 42:219–229.
  15. Huda W, Atherton JV, Ware DE, et al. An approach for the estimation of effective radiation dose at CT in pediatric patients. *Radiology* 1997; 203:417–422.
  16. Sharp C, Shrimpton JA, Bury RF. Diagnostic medical exposures: advice on exposure to ionizing radiation during pregnancy. Chilton Didcot, Oxon, United Kingdom: National Radiological Protection Board, 1998.
  17. Shrimpton PC, Jones DG, Hillier MC, Wall BF, Le Heron JC, Faulkner K. Survey of CT practice in the UK. 2. Dosimetric aspects—National Radiological Protection Board report 249. London, England: HMSO, 1991.
  18. Ryu JH, Swensen SJ, Olson EJ, et al. Diagnosis of pulmonary embolism with use of computed tomographic angiography. *Mayo Clin Proc* 2001; 76:59–65.
  19. Blachere H, Latrabe V, Montaudon M, et al. Pulmonary embolism reveal on helical CT angiography: comparison with ventilation-perfusion radionuclide lung scanning. *AJR Am J Roentgenol* 2000; 174: 1041–1047.
  20. Morisetti A, Tirone P, Luzzani F, et al. Toxicological safety assessment of iomeprol, a new x-ray contrast agent. *Eur J Radiol* 1994; 18(suppl 1):S21–S31.
  21. Value of the ventilation/perfusion scan in acute pulmonary embolism: results of the prospective investigation of pulmonary embolism diagnosis (PIOPED)—the PIOPED investigators. *JAMA* 1990; 263: 2753–2759.
  22. Erdman WA, Clarke GD. Magnetic resonance imaging of pulmonary embolism. *Semin Ultrasound CT MR* 1997; 18:338–348.
  23. Tengborn L, Bergqvist D, Matzsch T, et al. Recurrent thromboembolism in pregnancy and puerperium: is there a need for thromboprophylaxis? *Am J Obstet Gynecol* 1989;160:90–94.
  24. Speroff L, Glass RH, Kase NG. Oral contraception. In: *Clinical gynecologic endocrinology and infertility*. 5th ed. Baltimore, Md: Williams & Wilkins, 1994; 715–763.
  25. National Council on Radiation Protection. Exposure of the population in the United States and Canada from natural background radiation. Report 94. Bethesda, Md: National Council on Radiation Protection, 1987.
  26. Pregnancy and medical radiation: International Commission on Radiological Protection. *Ann ICRP* 2000; 30:1–43.